MR Imaging of the Scrotum

9

Michele Bertolotto, Francesca Cacciato,
Matilde Cazzagon, and Lorenzo E. Derchi

9.1 Introduction

Although ultrasonography remains the primary imaging modality in the diagnosis of scrotal pathology, magnetic resonance (MR) imaging may provide valuable additional information. Due to its increased panoramicity, it performs better with very large lesions, which are difficult to image in the limited field of view of the ultrasonographic probe. Another major strength over conventional ultrasound and Doppler modes is improved tissue characterization. Moreover, MR imaging can investigate heavily fibrotic or calcified testes, in which ultrasonography is inconclusive, and can detect flow in hypovascular lesions with a sensitivity rivaling that of contrast-enhanced ultrasonography [1].

9.2 Examination Technique

Scrotal MR imaging [2, 3] can be implemented with virtually every MR unit, even though image quality and signal-to-noise ratio is better with high-field-strength equipment. Susceptibility artifacts, which cause signal loss and image distortion at the air-tissue interface, are especially found at high field strength. To minimize this problem, it is recommended to use fast spin-echo instead of gradient echo sequences. Relatively low specific absorption rates (SAR) are used to minimize heating of the scrotum which, however, in a clinical setting is well below the threshold known to affect spermatogenesis in mammals [4].

9.2.1 Coil Selection

A circular surface coil can be used placed on the patient's lower pelvis and centered over the scrotum [5]. In our clinical practice, however, we prefer multichannel phased-array coils for parallel imaging, such as cardiac coils, which provide high-definition images with excellent signal-to-noise ratio and increased panoramicity. Appropriate positioning of the scrotum is important. The testes should be arranged to maintain nearly equal distance from the coil [5, 6]. The penis is kept upward and taped against the abdominal wall. Towels or sponges are placed between the thighs to minimize motion artifact. Respiratory compensation may be used to reduce motion artifact, but image quality obtained without respiratory compensation is high enough for the diagnosis with reduced acquisition time [7].

M. Bertolotto, MD (✉) • F. Cacciato • M. Cazzagon
Department of Radiology, University of Trieste,
Ospedale di Cattinara, Strada di Fiume 447,
Trieste 34149, Italy
e-mail: bertolot@units.it

L.E. Derchi
Dicmi-Radiologia, University of Genova,
Largo R. Benzi 8, Genoa 16132, Italy

R. Manfredi, R. Pozzi Mucelli (eds.), *MRI of the Female and Male Pelvis*,
DOI 10.1007/978-3-319-09659-9_9, © Springer International Publishing Switzerland 2015

9.2.2 Imaging Planes and Pulse Sequences

The testes are usually examined along the longitudinal and transverse axes. Coronal and axial acquisitions allow direct comparison of the two testes and evaluation of the spermatic cord [6]. Scanning along sagittal and oblique planes may be indicated in selected cases.

The scanning protocol varies depending on the clinical setting. In general, non-contrast-enhanced T1- and T2-weighted images are first obtained followed by contrast-enhanced T1-weighted images or dynamic contrast-enhanced scans if necessary. We commonly obtain high-resolution thin contiguous sections of 3–4 mm. Parallel imaging techniques are applied to reduce scan time by accelerating image acquisition. This eventually results in increased patient comfort and acceptability, decreased patient movement, and better image quality.

T1-weighted images provide anatomical information of the testis, epididymis, and spermatic cord. T2-weighted images are usually the most informative; they show a variety of tissue contrast depending on the echo time [2, 8]. A standard T2 contrast between the testes, epididymis, spermatic cord, and surrounding fat tissue is obtained with an echo time of about 100 ms; long echo times (250–350 ms) produce heavily T2-weighted images in which fluid displays very high signal intensity while the testes and epididymis have intermediate signal intensity. Diffusion-weighted imaging (DWI) of the scrotum is still on a stage of investigation [9–13]. It is usually performed along the axial plane using a single-shot, multislice, spin-echo planar sequence with b-values of 0 and 800–1,000 s/mm^2.

Contrast-enhanced MR imaging gives information on tissue perfusion. Comparison between the contrast enhancement of the right and left testes facilitates the evaluation of the affected-side testis with the unaffected-side testis serving as a normal control. Usually, high-resolution T1-weighted images with fat suppression are obtained before and after gadolinium contrast administration and image subtraction [14]. Dynamic contrast-enhanced imaging is indicated in selected cases only. It can be obtained in the coronal plane using fat-suppressed fast spin-echo images or ultrafast spoiled gradient echo sequences when a high temporal resolution is required, with the disadvantage of lower spatial resolution and increased artifacts. Image subtraction is recommended.

9.3 Normal Anatomy

The normal adult testes show intermediate- and high signal intensity on T1- and T2-weighted images, respectively [5, 6]. Intermediate signal intensity is displayed on heavily T2-weighted images. On DWI images the normal testes present homogeneous high signal intensity (Fig. 9.1). Aging is associated with structural and functional alterations resulting in decreased signal restriction [15]. The mediastinum testis appears as a low-signal-intensity band along the long axis of the testis. On heavily T2-weighted images, fine fibrous septa are often seen as thin linear structures of low signal intensity extending from the mediastinum testis and dividing the lobules. The tunica albuginea and the visceral layer of the tunica vaginalis are stuck together showing low signal intensity in all sequences [5, 6, 16]. The signal intensity of the epididymis is similar to that of the testis on T1-weighted images but lower on T2-weighted images [5, 6, 17]. The vas deferens can be traced from the tail of the epididymis to the spermatic cord on T2-weighted images.

The fluid between the visceral and the parietal layers of the tunica vaginalis shows high and very high signal intensity on T2- and heavily T2-weighted images, respectively [5, 6].

9.4 Congenital Abnormalities

MR imaging is the imaging modality of choice in investigating patients with ambiguous genitalia, which are usually associated with complex malformations of the genitourinary tract. The most common isolated abnormalities of the scrotal content are undescended testis and congenital hydro-

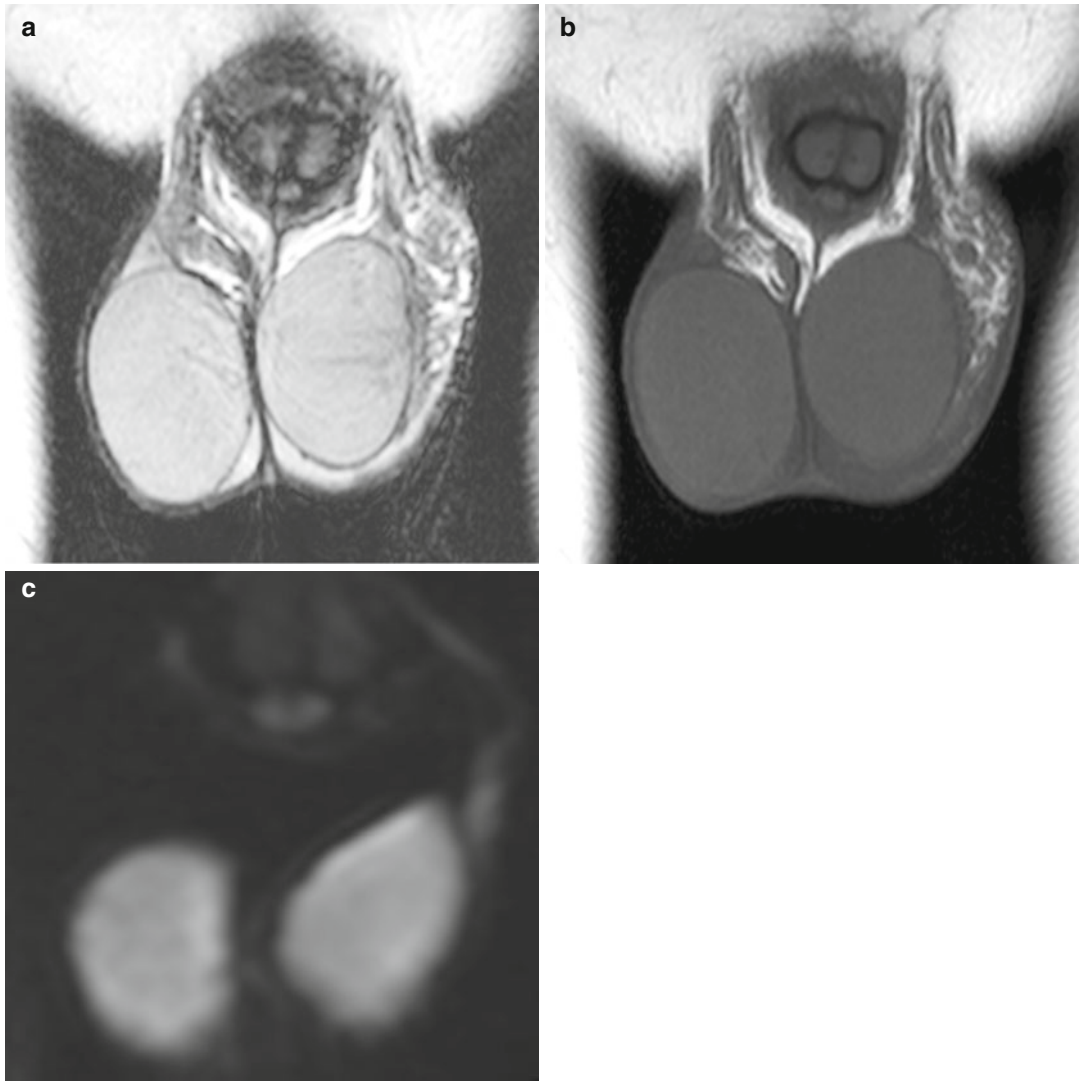

Fig. 9.1 Appearance of the normal testes on MR imaging. Coronal images. (**a**, **b**) The testes show high signal intensity on T2- and intermediate signal intensity on T1-weighted images, respectively. The tunica albuginea has low signal intensity in all sequences. (**c**) Diffusion-weighted image ($b = 1{,}000$ s/mm^2) shows signal restriction of the testicular parenchyma

celes. Bell-clapper deformity is difficult to be detected. Polyorchidism and adrenal rests are rare.

9.4.1 Undescended Testis

Undescended testis is the most common genitourinary anomaly with a prevalence at birth of 2–5 % and up to 30 % in preterm infants. Approximately 2:3 undescended testes will spontaneously descend within the first months of life, with a prevalence at the age of 1 year of 0.8 %. The testis may be located at any point along the descent route from the retroperitoneum to the external inguinal ring [18]. It can be ectopic, but in general it is found along the normal path of descent: approximately 70 % in the inguinal canal, 20 % in the prescrotal region just beyond the external inguinal ring, and the remaining in the abdomen. About 3–5 % of patients with undescended testis

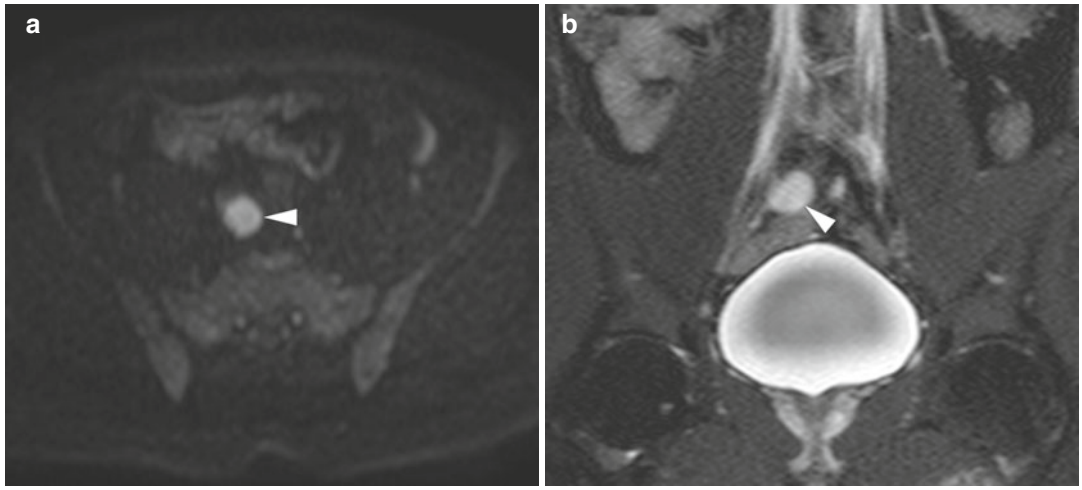

Fig. 9.2 An undescended testis located in the abdomen near the right iliac vessels. (**a**) Axial diffusion-weighted image ($b = 800$ s/mm^2) identifies the retained testis as a lesion with signal restriction (*arrowhead*). (**b**) Coronal T2-weighted image confirming the location of the testis adjacent to the right iliac vessels (*arrowhead*)

have congenital absence of the testis. It is conceivable that in most cases, the testis was originally present during fetal life and then regressed.

The major complications of cryptorchism are malignant degeneration, infertility, torsion, and bowel incarceration because of an associated indirect inguinal hernia. Tumors are far more common in an undescended testis than in a normally positioned testis.

Imaging is indicated to search for the location of the cryptorchid testis to evaluate its size and to seek for parenchymal lesions. The cryptorchid testis is usually smaller relative to the normally located testis because of testicular dystrophy and degeneration [19].

Ultrasonography can reliably detect testicles located in the inguinal canal or between the external inguinal ring and the scrotal neck. Detecting the testicle in intra-abdominal locations is often difficult or even impossible. MR imaging allows detecting the testis not only in the inguinal canal but also in the abdomen. High abdominal testes, however, may be difficult to identify, and a recent meta-analysis of an American pediatric group shows a low sensitivity [20]. DWI performed at high b-values (800–1,000 s/mm^2) improves visualization of the undescended testis which appears hyperintense in most of cases [13] (Fig. 9.2). Severely atrophic testes, however, may show low signal intensity on diffusion-weighted imaging [21] (Fig. 9.3).

9.4.2 Congenital Hydrocele

Congenital hydrocele occurs when there is incomplete closure of the processus vaginalis. It is very common in newborn but is encountered in less than 1 % of adults. The patent processus vaginalis permits flow of peritoneal fluid into the scrotum. Indirect inguinal hernias can be associated. There are two subtypes of congenital hydrocele: the encysted type, also called spermatic cord cyst, with no communication with the peritoneum and with the tunica vaginalis, and the funicular type, also called funiculocele, which communicates with the peritoneum at the internal ring but does not surround the testis.

Either ultrasonography or MR imaging can be used to evaluate congenital hydrocele. On ultrasound, it appears as an anechoic fluid collection surrounding the anterolateral aspects of the testis extending to the inguinal canal or as a well-demarcated anechoic mass, associated with either a patent or a closed internal ring, separated from the testis and epididymis which are displaced inferiorly. On MR imaging hydrocele is homogeneous and hypointense on T1-weighted images

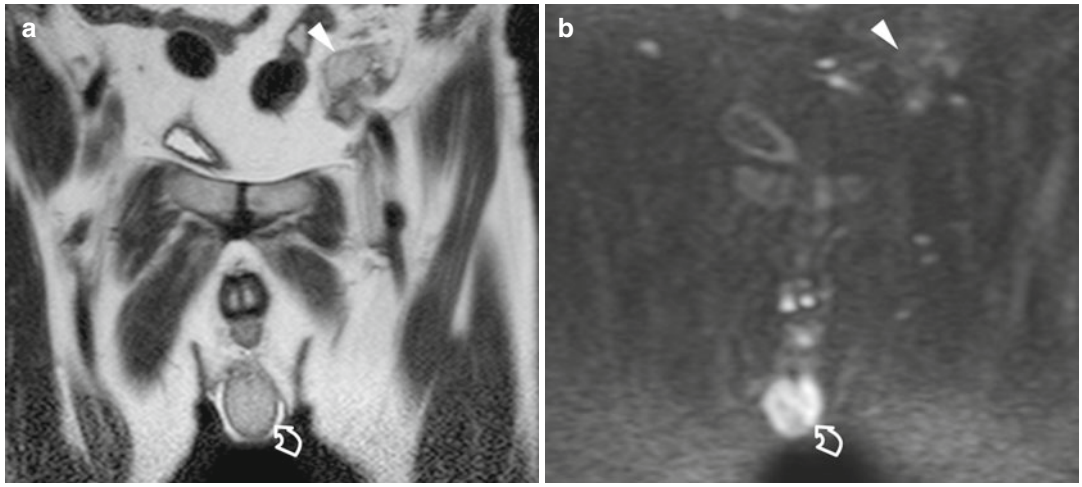

Fig. 9.3 An undescended testis located in the abdomen near the left iliac vessels. (**a**) Coronal T2-weighted image showing a normally descended right testis (*curved arrow*) and a small left testis adjacent to the left iliac vessels (*arrowhead*). (**b**) Coronal diffusion-weighted image ($b = 1{,}000$ s/mm^2) fails to show signal restriction of the retained testis (*arrowhead*), which was markedly dystrophic and poorly vascularized at surgery (*arrowhead*). The normally descended right testis (*curved arrow*) displays signal restriction

and hyperintense on T2-weighted images, characteristic of fluid. Occasionally, septations are identified, although prominent septations should suggest a hematocele or pyocele. Patency of the processus vaginalis with entry of peritoneal fluid into the scrotal sac is best demonstrated in heavily T2-weighted images.

9.4.3 Bell-Clapper Deformity

Failure of the normal posterior anchoring of the epididymis and testis is called bell-clapper deformity because it leaves the testis free to swing and rotate within the tunica vaginalis of the scrotum like the clapper inside of a bell. It is a common precondition for testicular torsion, with a 12 % incidence in an autopsy series.

Bell-clapper deformity itself is hard to be detected by imaging. A suggestive feature is the abnormal direction of the long axis of the testis on the axial plane, in the right-to-left or anterior-posterior direction with the epididymis right upon the testis (Fig. 9.4). The deformity is more often recognized in heavily T2-weighted images when hydrocele is present and the tunica vaginalis completely encircles the epididymis, distal spermatic cord, and testis rather than attaching to the posterolateral aspect of the testis.

9.4.4 Polyorchidism

Polyorchidism is a rare congenital abnormality where more than two testes are present which may have separate or common spermatic cords and epididymis. Although three testes is the most common form, as many as five have been reported. In approximately 75 % of cases, the supernumerary testes are intrascrotal. Of the remaining cases, 20 % of the supernumerary testes are inguinal and 5 % retroperitoneal. On ultrasonography the accessory testis presents with the same echogenicity, echotexture, and vascular pattern as the normal testes. On MR imaging it has the same signal characteristics as the normal testes: intermediate signal intensity on T1-weighted images, high signal intensity on T2-weighted images, and hyperintensity on DWI (Fig. 9.5). Thanks to its panoramicity and improved tissue characterization, MR imaging is helpful in making a definitive diagnosis in case of equivocal ultrasound findings or extrascrotal testes [22].

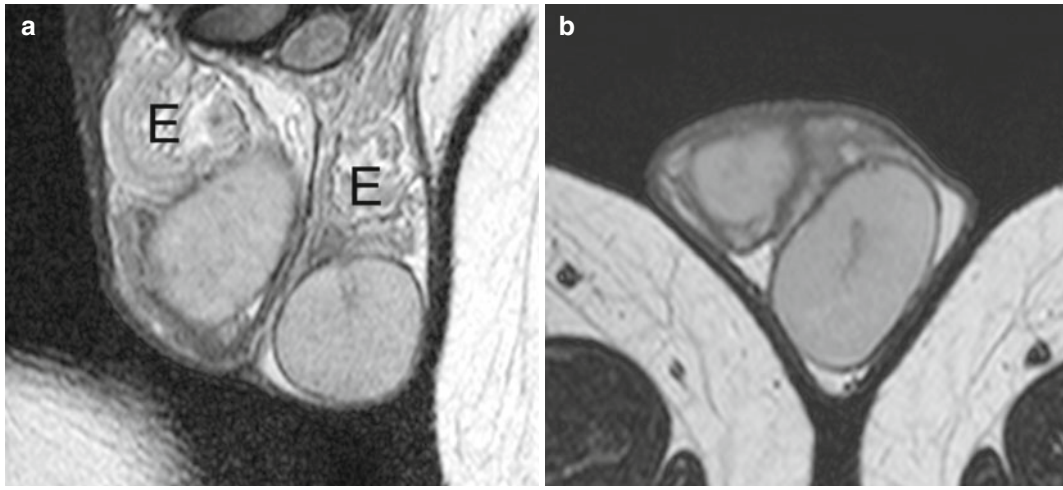

Fig. 9.4 Surgically proved bell-clapper deformity. The patient had several episodes of acute scrotal pain on both sides which released spontaneously, interpreted as recurrent episodes of low-degree torsion with spontaneous detorsion. Coronal (**a**) and axial (**b**) T2-weighted images show the major axis of the testes laying on an axial plane, the right testis in right-to-left direction, the left in anterior-posterior direction. The epididymis (*E*) is right upon the testes in both sides

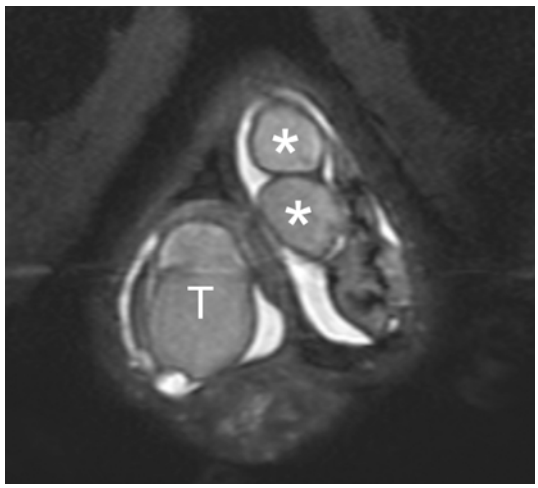

Fig. 9.5 Polyorchidism. Oblique-coronal T2-weighted image shows a single testis (*T*) on the right hemiscrotum and two testes (*asterisks*) in the left hemiscrotum

9.4.5 Testicular Adrenal Rests

Testicular adrenal rests derive from the hyperplasia of aberrant adrenal cortical tissue that descends during prenatal life with the testes or ovary. In approximately 8 % of patients with congenital adrenal hyperplasia, the elevated levels of serum adrenocorticotropic hormone stimulates these rests to grow. They are bilateral in more than 80 % of cases, usually presenting as palpable masses inside of or close to the mediastinum testis.

Testicular adrenal rests present on ultrasound as unilateral or bilateral lobulated masses with variable echogenicity located within or adjacent to the mediastinum testis. Acoustic shadowing may be due to fibrotic changes or calcifications. Lesions are isointense to the surrounding normal tissue of the testis on T1-weighted images and hypointense to the surrounding normal tissue of the testis on T2-weighted images with and without fat suppression. Strong enhancement is demonstrated after gadolinium administration.

9.5 Ischemic Disorders

The mainstay of imaging ischemic scrotal disorders is color Doppler ultrasonography. In high-degree torsion non-enhancement of the testis after gadolinium administration has been reported as highly sensitive and specific for torsion [14], but MR imaging is more expensive and time-consuming than color Doppler ultrasonography and therefore has no or minimum practical role in the setting of acute scrotal pain. In low-degree torsion perfusion is reduced compared with the healthy contralateral testis [23]. In acute

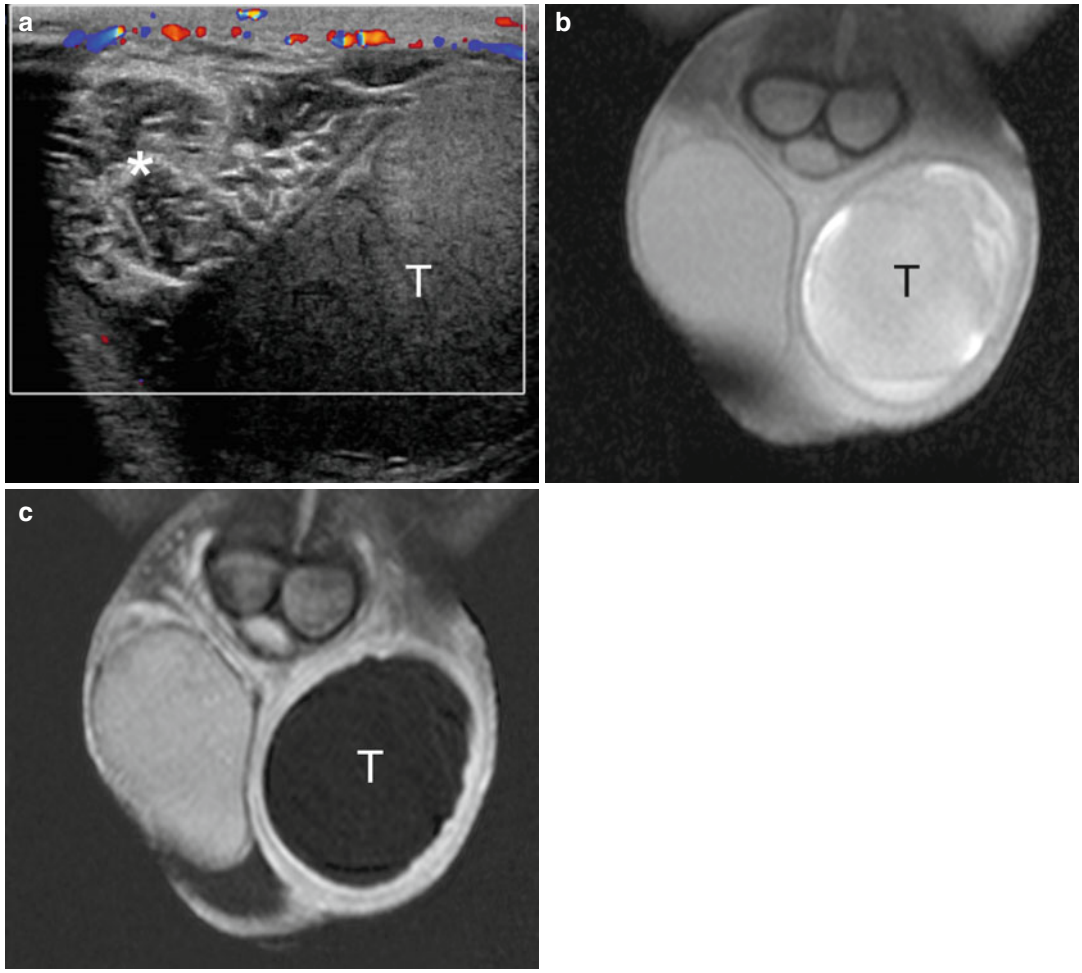

Fig. 9.6 Long-standing high-degree left testicular torsion. (**a**) Color Doppler interrogation shows an avascular left testis (*T*) and a twisted spermatic cord (*asterisk*). The paratesticular tissues display increased vascularization. (**b**) T1-weighted coronal image with fat suppression shows inhomogeneous left testis (*T*) with high signal intensity due to hemorrhagic changes. (**c**) Gadolinium-enhanced subtracted image showing complete lack of vascularization of the left testis (*T*) and slight hyperemia of the surrounding tissues

testicular torsion, the testis has normal signal intensity on both T1- and T2-weighted images and high signal intensity on DWI [9]. The twisted spermatic cord is best demonstrated on transaxial T2-weighted and contrast-enhanced images [24]. In the subacute and chronic stages, the signal intensity of the testis changes due to necrosis and hemorrhagic components (Fig. 9.6).

9.5.1 Torsion of the Appendages

The normal appendages are typically seen only when hydrocele is present [25–27]. They usually display intermediate signal intensity on T2-weighted images. In appendiceal torsion, a twisted and swollen appendage is usually seen as a hyperintense oval structure on T2-weighted images lacking intralesional enhancement with ring-like perilesional enhancement on dynamic subtraction contrast-enhanced images [2, 28].

9.5.2 Segmental Testicular Infarction

MR imaging has been claimed as a problem-solving technique in doubtful cases of segmental

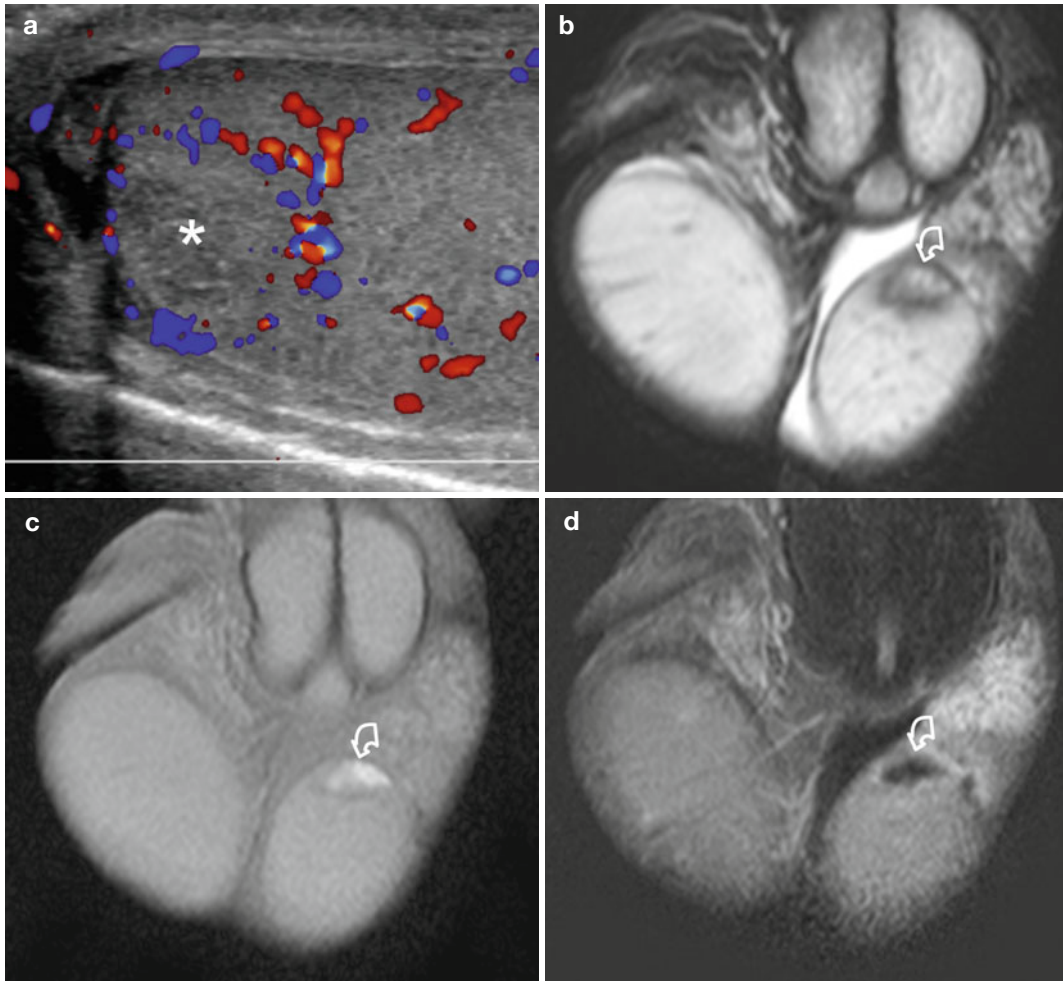

Fig. 9.7 Segmental testicular infarction. Patient presenting with acute left scrotal pain. (**a**) Color Doppler interrogation shows an avascular, slightly hypoechoic area (*asterisk*) in the upper pole of the left testis with perilesional hypervascularization. (**b**) T2-weighted coronal image showing the lesion (*curved arrow*) with inhomogeneous signal intensity. (**c**) T1-weighted image showing the hyperintense lesion (*curved arrow*) due to hemorrhagic changes. (**d**) Gadolinium-enhanced subtracted image shows lack of vascularization of the lesion (*curved arrow*) and slight perilesional hypervascularization

testicular infarction [29, 30]. On T1-weighted MR images, infarcts may appear isointense to the surrounding normal testicular parenchyma, occasionally with foci of high signal intensity due to hemorrhage.

On T2-weighted images, the signal intensity is variable. The lesion is avascular after gadolinium contrast administration (Fig. 9.7), often with an enhancing perilesional rim in subacute infarction [29, 31]. Although segmental testicular infarction presents with characteristic MR features, this investigation is not commonly performed in our clinical practice, as similar information is provided by contrast-enhanced ultrasonography which is quicker and with a lower cost [32].

9.6 Inflammation

MR imaging provides a panoramic view of the extension of the disease to adjacent organs in severe scrotal inflammation. Involvement of the perineum

and/or abdominal region can be investigated. MR imaging enables a diagnosis of postinflammatory testicular ischemia, testicular hemorrhagic and necrotic changes, epididymo-orchitis with abscess formation, and intrascrotal fistulas [33]. In acute epididymitis the enlarged epididymis has increased signal intensity relative to the normal side on T2-weighted images and clearly shows intense contrast enhancement on dynamic subtraction contrast-enhanced images. Abscesses are typically hypointense on T1-weighted images, hyperintense on T2-weighted images, and display high signal intensity on DWI images. They do not enhance, while the surrounding tissues show avid enhancement.

9.7 Testicular Masses

Not all intratesticular lesions are tumors, and not all testicular tumors are malignant. Granulomata, focal orchitis, fibrous pseudotumors, and spontaneous hematomas are often difficult to differentiate from tumors on ultrasound examination. In many cases, however, it is suggested that the diagnosis integrates the history of the patient, clinical presentation, and the superior capability of MR imaging for tissue characterization and evaluation of intralesional flows.

The patient's age at presentation is important. Germ cell tumors are prevalent in the young while lymphomas in the elderly, and some histotypes are much more prevalent in prepuberal than in puberal boys. Clinical correlation is vital: many nonneoplastic intratesticular conditions are likely to manifest with acute scrotum. One needs to be cautious, however, because tumors can also occasionally manifest with pain. A history of fever or trauma may suggest a nonneoplastic origin as well. Tumor markers often help in the differential diagnosis between testicular tumors and nonneoplastic lesions. Normal serum tumor markers, however, do not rule out testicular neoplasms. In any case, traumatic and inflammatory changes evolve rapidly; if a nonneoplastic pathology is suspected, a short-term follow-up examination will likely allow differential diagnosis with tumor.

9.7.1 Dilated Rete Testis

Tubular ectasia of the rete testis is a benign nonneoplastic condition thought to result from partial or complete obliteration of the efferent ducts. It is more common in men over the age of 55 years, often bilateral, and frequently associated with spermatoceles.

Using modern ultrasonographic equipment, a tubular ectasia of the rete testis is characterized in virtually all patients; in case of doubt, however, MR can show the dilatation of multiple small tubules of the rete testis appearing hyperintense on T2-weighted and heavily T2-weighted images. After gadolinium administration no internal enhancement is seen [16].

9.7.2 Testicular Epidermoid Cyst

The classic ultrasonographic appearance of testicular epidermoid cyst is the "onion ring" pattern, consisting in alternating rings of low and high echogenicity, which represent layers of keratinized squamous epithelium. This appearance is virtually pathognomonic, but epidermoid cysts with an atypical appearance may be difficult to differentiate from tumors. On MR imaging an epidermoid cyst typically shows on T2-weighted images alternating zones of high- and low signal intensity [1, 34, 35] and signal restriction on DWI [11]. This appearance, however, is not constant (Fig. 9.8). Signal intensity on T1-weighted images is variable. No matter the imaging features, epidermoid cysts do not demonstrate internal flow on Doppler interrogation nor enhancement after gadolinium administration [16].

9.7.3 Spontaneous Testicular Hematoma

Spontaneous intratesticular hematoma is a rare entity with few reports in the literature, mimicking a neoplasm on grayscale ultrasonography. Diagnosis of a nonneoplastic condition, however, is suggested as the lesion lacks vascularization on color Doppler interrogation and contrast-enhanced

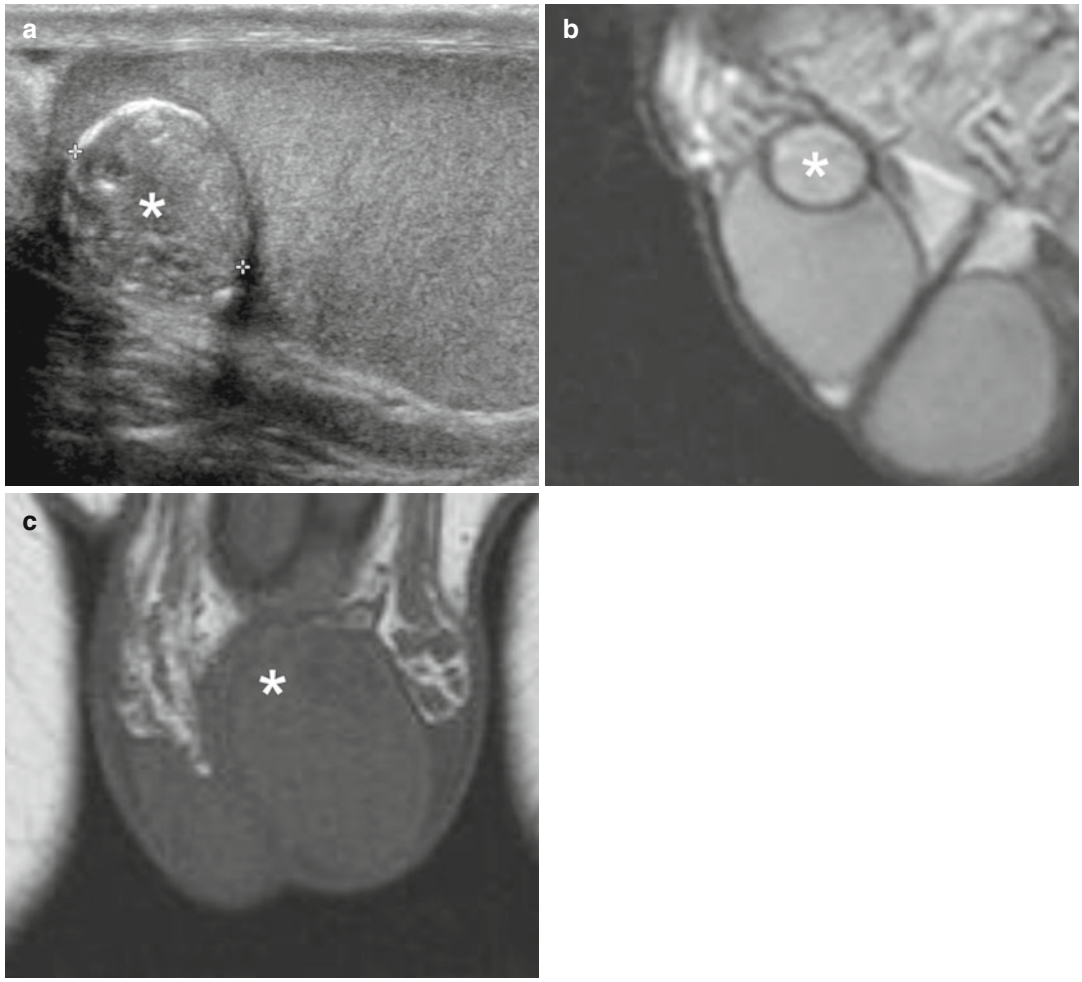

Fig. 9.8 Epidermoid cyst presenting as a palpable nodule of the left testis. (**a**) Grayscale ultrasonography showing a slightly inhomogeneous lesion isoechoic to the surrounding normal tissue of the testis, with a few wall calcifications (*asterisk*). (**b**) Sagittal T2-weighted image shows a slightly hyperintense nodule (*asterisk*) with hypointense wall. (**c**) Coronal T1-weighted image showing the lesion (*asterisk*) isointense to the surrounding normal tissue of the testis, which was completely avascular after gadolinium contrast administration (not shown)

ultrasonography [36, 37]. MR imaging confirms the diagnosis showing a lesion with the characteristic signal changes of blood. No enhancement is seen after gadolinium contrast administration (Fig. 9.9). Follow-up is recommended to ascertain lesion size reduction and signal intensity changes over time of the blood content.

9.7.4 Fat-Containing Masses

Testicular lipoma is a rare condition now being increasingly reported secondary to the widespread use of scrotal sonography [38–40]. On ultrasonography lipoma usually consists of a homogeneously hyperechoic non-shadowing lesion without flow on color Doppler interrogation. The diagnosis is confirmed on MR imaging which shows the signal intensity characteristics of fat in all sequences [22] (Fig. 9.10).

Testicular lipomatosis is a recently described entity occurring in patients with Cowden disease and in Bannayan-Riley-Ruvalcaba syndrome [41] in which nonneoplastic fat-containing hamartomas are seen. On ultrasonography testicular lipomatosis presents with multiple non-shadowing, uniformly hyperechoic small round foci of various sizes in both testes [42]. Although virtually

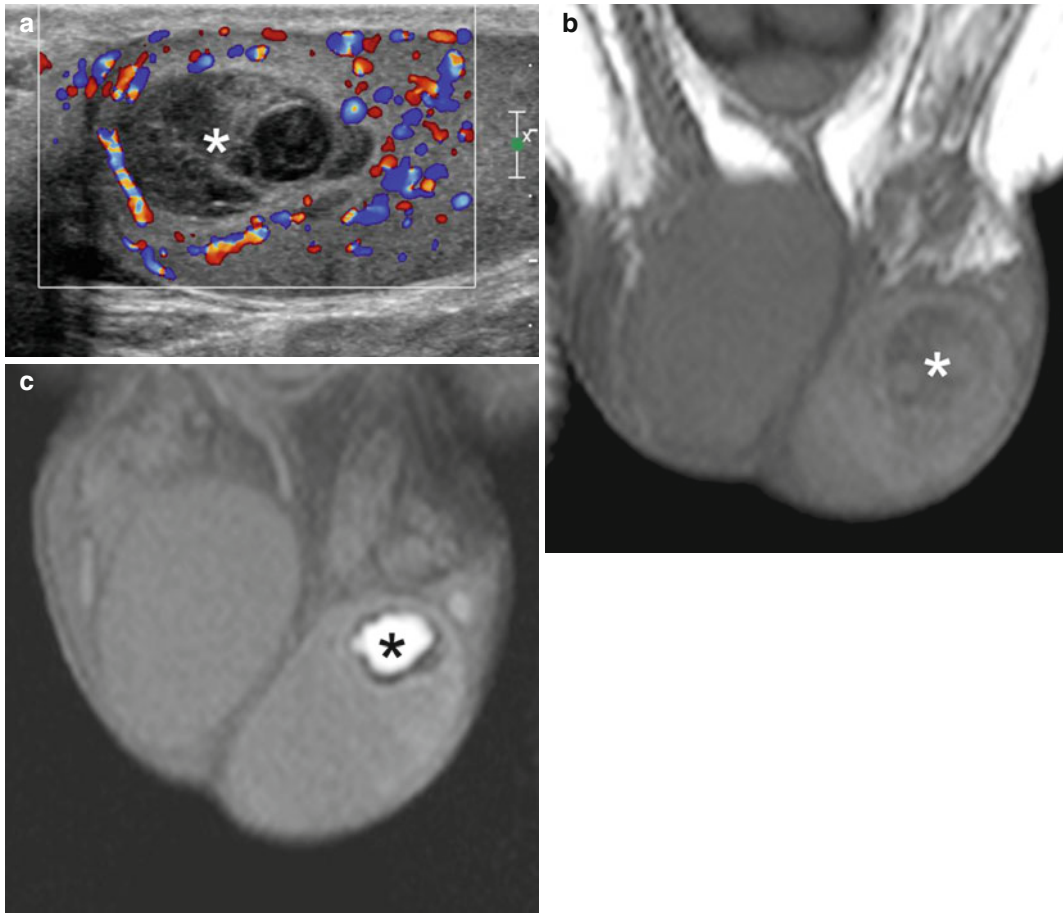

Fig. 9.9 Spontaneous testicular hematoma. The patient presented with acute left scrotal pain for 3 h with no history of trauma. (**a**) Color Doppler interrogation shows an inhomogeneously hypoechoic left testicular lesion lacking vascularization (*asterisk*). (**b**) Coronal T1-weighted image obtained within 24 h after ultrasonography shows an inhomogeneous isointense lesion (*asterisk*) which was avascular after gadolinium contrast administration (not shown). (**c**) Follow-up MR investigation obtained 2 months after the previous study. Coronal T1-weighted image shows a hyperintense lesion (*asterisk*) which is reduced in size, characterized by hypointense rim due to blood degradation

diagnostic of testicular lipomatosis in the context of known Cowden disease, this pattern may also be due to fibrotic changes and other conditions. MR imaging allows differential diagnosis showing multiple foci in both testes with the signal intensity characteristics of fat [43].

9.7.5 Calcifying, Sclerosing, and Fibrotic Lesions

Heavily calcified adrenal rests [3], epidermoid cysts with peripheral and intralesional calcifications, calcified intratesticular hematomas, and calcifying, sclerosing, and fibrotic tumors such as cavernous hemangioma [44], large-cell calcifying Sertoli cell tumor [34], and sclerosing Sertoli cell tumor [45] cannot be investigated effectively with ultrasonographic modes due to back attenuation. MR imaging is indicated in these patients to evaluate the lesion, attempt tissue characterization, and investigate whether it is vascularized or not [45].

9.7.6 Heavily Calcified and Strongly Heterogeneous Testes

MR imaging is indicated to rule out clinically suspected testicular lesions in patients with heterogeneous testicular parenchyma on

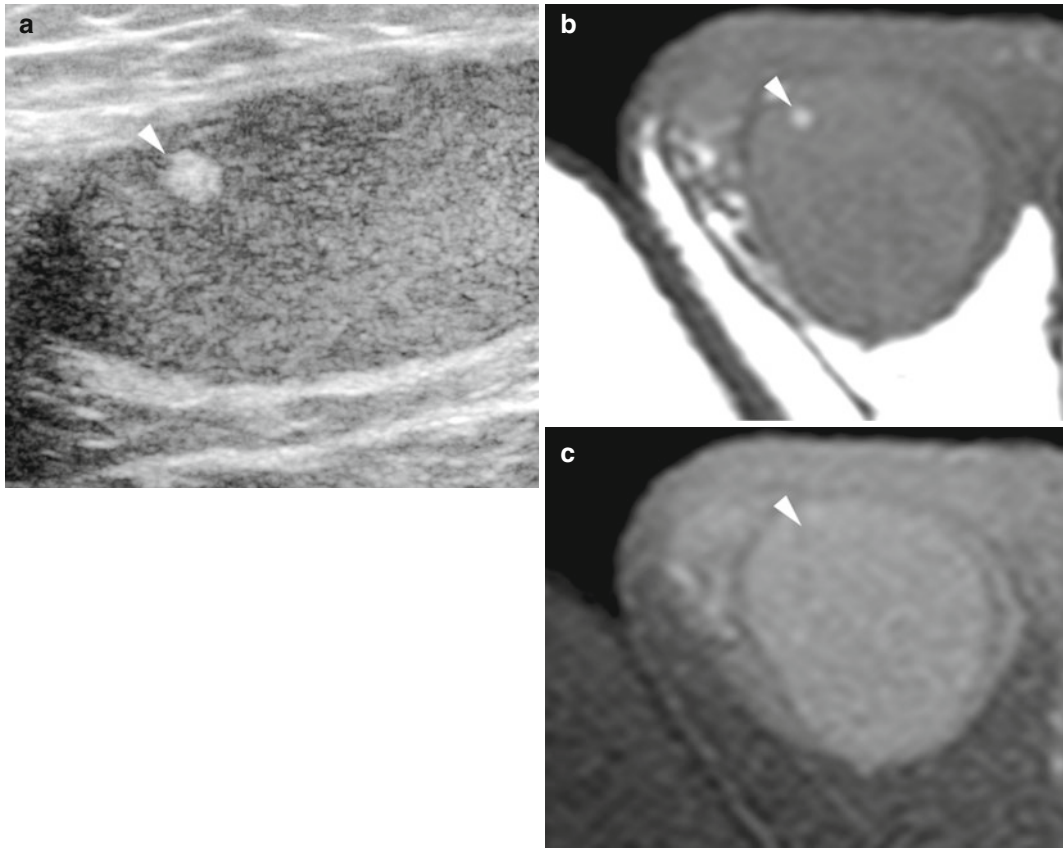

Fig. 9.10 Testicular lipoma. (**a**) Grayscale ultrasonography shows a small hyperechoic right testicular lesion (*arrowhead*). (**b**) The lesion (*arrowhead*) is hyperintense on axial T1-weighted image and displays signal loss in the T1-weighted fat-suppressed image (**c**)

ultrasonography (Fig. 9.11); testicular fibrotic changes either after inflammation, surgery, or trauma; multiple testicular calcifications; or microlithiasis with heavily calcified testes. Fibrosis, in particular, can be very worrisome on ultrasonography, but the low signal intensity in T1- and T2-weighted images, sometimes radiating from the mediastinum, is indicative of a benign lesion.

9.7.7 Other Testicular Neoplasms

A recent study shows that T2-weighted and contrast-enhanced T1-weighted images have the potential to characterize seminomatous from nonseminomatous testicular neoplasms [46]. A seminoma usually presents as a rounded or multinodular sharply defined lesion with predominantly low signal intensity on T2-weighted images. Fibrovascular septa showing greater enhancement than tumor tissue after gadolinium administration are typically detected. Nonseminomatous tumors usually appear as heterogeneous masses on T2-weighted images with heterogeneous enhancement after gadolinium administration. In our experience, however, this appearance is far from sensitive or specific. Dynamic contrast-enhanced MR imaging defines three different types of time-intensity curves. In type I the signal gradually continues to increase; in type II an initial upstroke is followed by either a plateau or a gradual increase in the late phase; in type III an initial upstroke is followed by gradual washout. The normal testis is characterized by an enhancement with a type I curve, while type II is prevailing in benign lesions and type III in

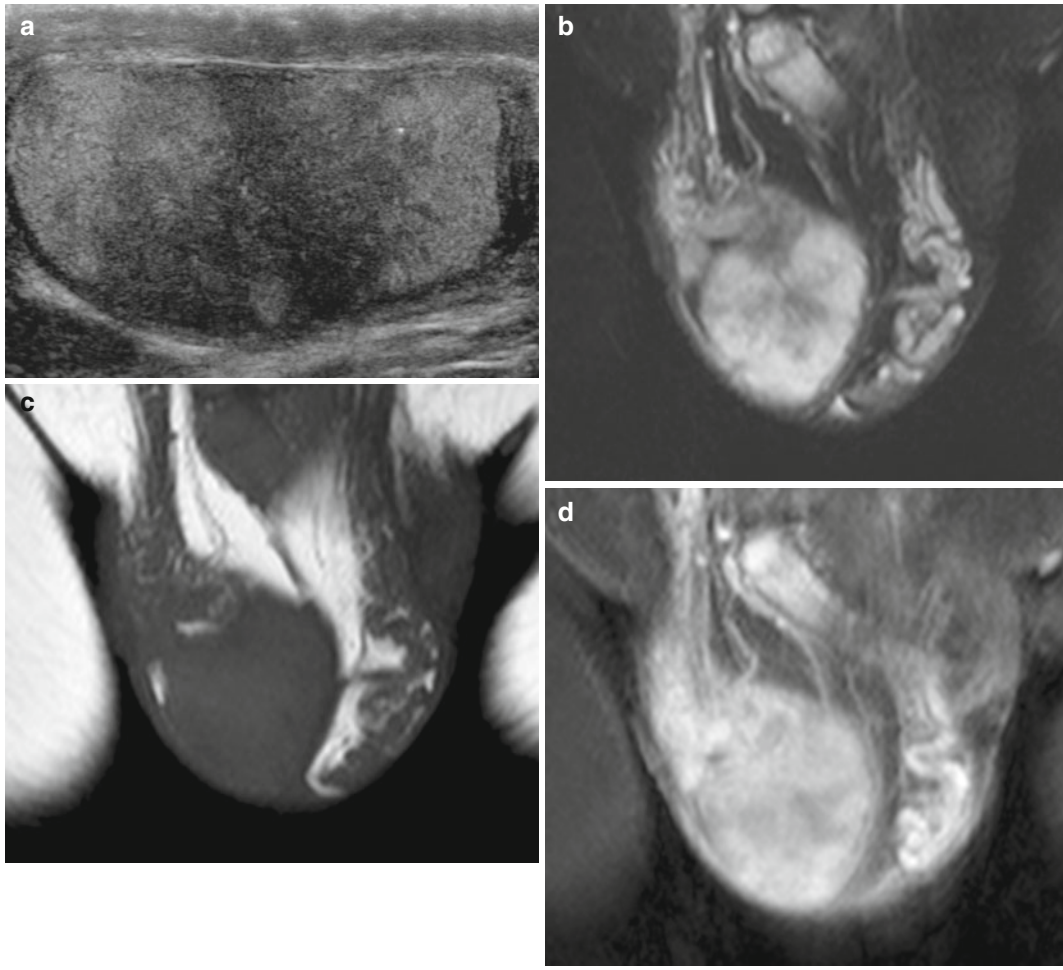

Fig. 9.11 MR investigation of a patient with inconclusive ultrasonographic scan. (**a**) Grayscale ultrasonography shows a markedly inhomogeneous right testis. (**b–d**) T2-weighted, T1-weighted, and T1-weighted fat-suppressed images obtained after gadolinium contrast administration allow to ruling testicular lesions

malignant lesions [47]. Malignant tumors often show increased signal restriction in DWI compared to the normal testis [10]. Despite these promising results, in the common clinical practice the evaluation of time-intensity curves and ADC values is unable to differentiate benign and malignant testicular lesions clearly.

9.8 Paratesticular Lesions

Approximately 70 % of paratesticular tumors are benign. Ninety percent are found in the spermatic cord followed by the epididymis and testicular tunicae. Lipoma is the most common tumor of the spermatic cord in adults followed by leiomyoma, lymphangioma, and angioleiomyoma [16]. While liposarcoma is the most common malignant neoplasm of the spermatic cord in adults, rhabdomyosarcoma is the most common paratesticular neoplasm in children and adolescents. Other sarcomas are rare. Adenomatoid tumor accounts for approximately one-third of all neoplasms of the paratesticular tissues. This benign lesion is more frequent in the tail of the epididymis but may develop anywhere in the epididymis and also in the spermatic cord and tunica albuginea, where it can mimic a testicular lesion.

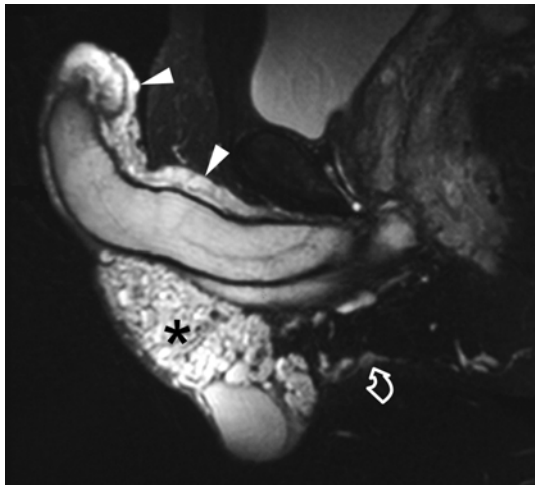

Fig. 9.12 Giant penoscrotal cavernous hemangioma. T2-weighted sagittal MR image showing a high-signal-intensity lesion involving the scrotum (*asterisk*), the anterior portion of the perineum (*curved arrow*), and the dorsal aspect of the penis (*arrowheads*)

Tumors of the tunicae and of the scrotal wall are very rare. The most common are malignant mesothelioma of the tunica vaginalis of the testis and scrotal hemangioma. Metastatic deposits are seen in patients with a known malignancy in an advanced stage.

9.8.1 Scrotal Hemangioma

In patients with large scrotal hemangiomas, MR imaging is indicated to determine the anatomic extension of the lesion to the penis, scrotum, and anterior perineum. The lesion appears as a lobulated scrotal mass with intermediate signal intensity on T1-weighted images and high signal intensity on T2-weighted images (Fig. 9.12). Focal areas of signal void consistent with a thrombus can be recognized.

9.8.2 Extratesticular Epidermoid Cysts

Extratesticular epidermoid cysts are rare [48]. Inflammation leads to calcification of the cystic wall with subsequent calcification of the content. Complete local excision is considered the treatment of choice.

At ultrasonography the appearance of extratesticular epidermoid cysts varies from anechoic to hyperechoic depending on their content. Calcified lesions are echogenic with back attenuation. On MR imaging extratesticular epidermoid cysts are usually thin-walled, hypointense on T1-weighted images, and hyperintense on T2-weighted images and show signal restriction on DWI images. However, they may show heterogenous intensity on both T1- and T2-weighted images due to inner dense keratinous materials. Signal intensity is low in heavily calcified lesions. Gadolinium-enhanced images usually show only peripheral wall enhancement (Fig. 9.13).

9.8.3 Fibrous Pseudotumor

Fibrous pseudotumor represents a benign reactive fibrous proliferation that results in one or several paratesticular nodules, usually arising from the tunica vaginalis. It is the third most common extratesticular mass after lipoma and adenomatoid tumor. Lesions as large as 8 cm have been reported. There is hydrocele in 50 % of cases. Local excision can be performed and orchiectomy avoided. On ultrasonography, the typical appearance of fibrous pseudotumor is a hypoechoic mass or several tunical masses, sometimes with internal calcifications. On MR imaging, fibrous pseudotumors show uniformly intermediate-to-low signal intensity on T1-weighted images and are markedly hypointense on T2-weighted images (Fig. 9.14), with slow but persistent enhancement [22].

9.8.4 Other Extratesticular Tumors

Fat-containing lesions can be characterized on MR imaging (Fig. 9.15), but lipoma may be difficult to differentiate from liposarcoma. Lymphoma is suspected when a diffuse infiltration of the spermatic cord by tumor tissue is seen, surrounding the spermatic vessels whose course and caliber are preserved. Tumor tissue is

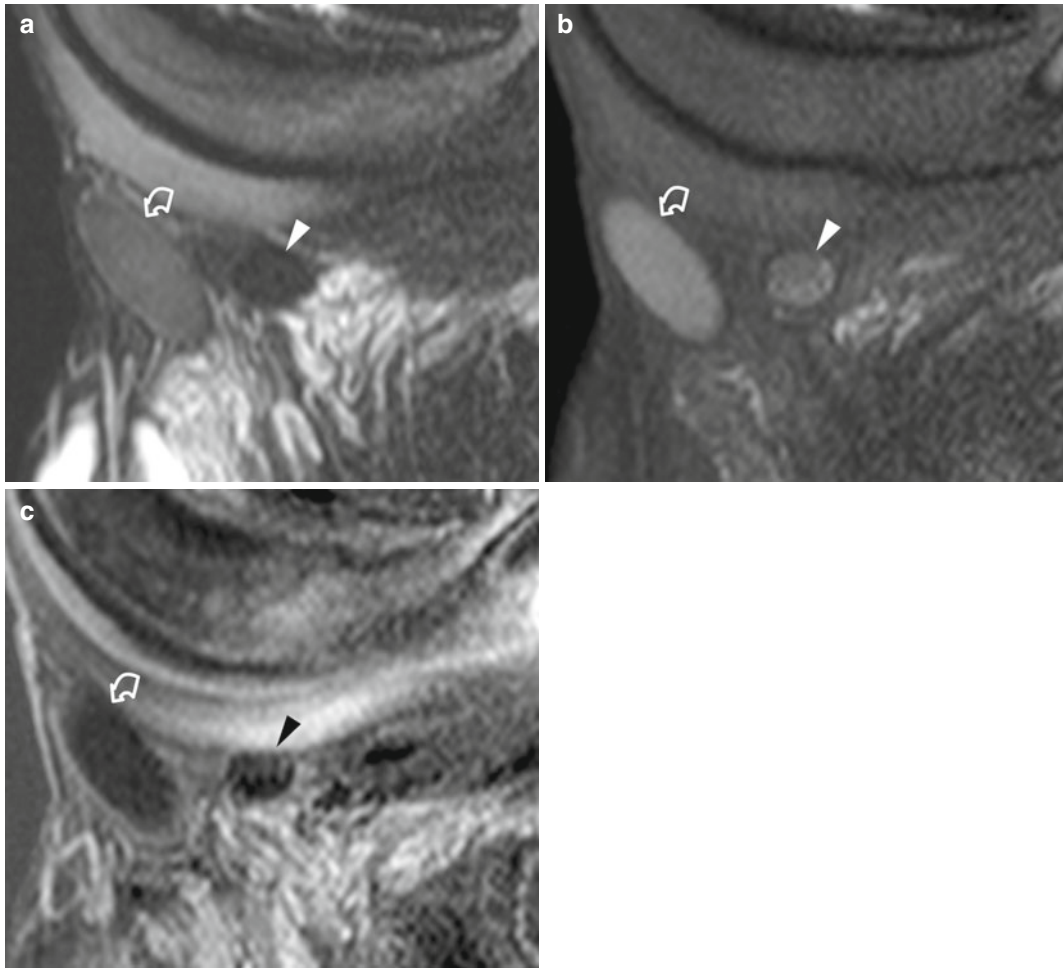

Fig. 9.13 Epidermoid cysts of the scrotal wall. T2-weighted (**a**) and T1-weighted sagittal images with fat suppression (**b**) show two well-demarcated masses, the larger with intermediate signal intensity on T2-weighted images (*curved arrow*) and the smaller with low signal intensity (*arrowhead*). Both lesions display relatively high signal intensity on T1-weighted images. (**c**) Subtraction images obtained after gadolinium contrast administration show no enhancement with minimum enhancement of the cystic wall (*curved arrow*). The smaller nodule (*arrowhead*) was partially calcified

markedly hypervascular after gadolinium contrast administration, homogeneously hypointense on T2-weighted images, isointense to the surrounding normal tissue of the testis on T1-weighed images, and lacking fat tissue [49]. High signal intensity is found on diffusion-weighted images (DWI), as occurs for lymphomas elsewhere in the body.

The MR imaging appearance of the other extratesticular scrotal tumors is not specific. Scrotal metastatic deposits are indistinguishable from primary neoplasms. A preliminary investigation suggests that hypointensity on DWI and increased ADC are in favor of benign paratesticular lesions [10].

9.9 Inguinal-Scrotal Hernia

Though physical examination and ultrasonography allow for accurate diagnosis in most cases, MR examination can be indicated in patients with inconclusive findings. Fat tissue such as the omentum and mesentery, protruding through the inguinal canal, usually shows high signal intensity on T1-weighted images and low signal

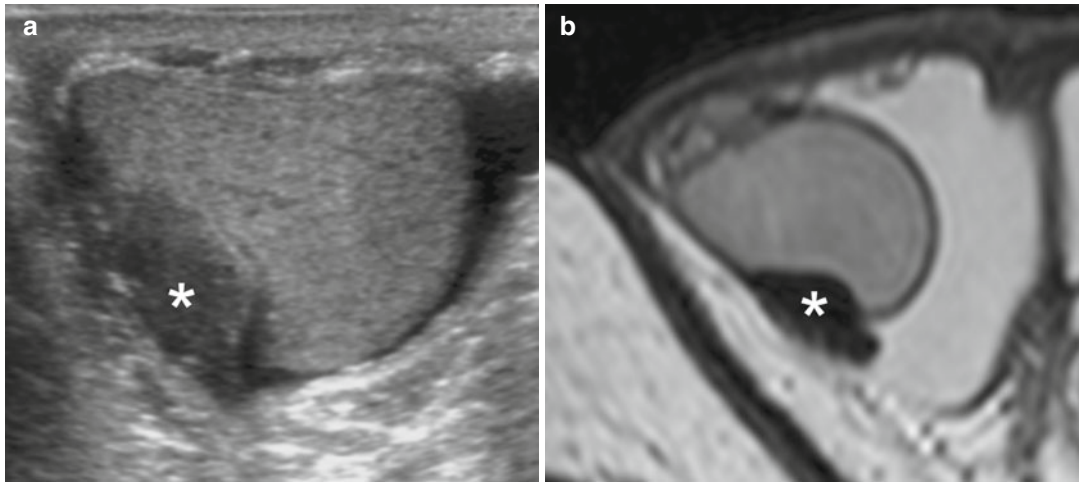

Fig. 9.14 Fibrous extratesticular pseudotumor. (**a**) Ultrasonography shows a hypoechoic lesion (*asterisk*) causing compression of the testicular parenchyma arising from the tunica albuginea or from the visceral lamina of the tunica vaginalis. (**b**) T2-weighted axial image confirms the extratesticular location of the low-signal-intensity lesion (*asterisk*)

intensity on T1- and T2-weighted images with fat suppression. Vessels of the omentum and/or mesentery appear as curvilinear structures. Herniation of bowel loops and of other viscera, such as the urinary bladder, can be investigated.

9.10 Varicocele

Although color Doppler ultrasonography is the modality of choice for imaging varicocele, this pathological condition may be an incidental finding on MR imaging in patients investigated for other purpose. The MR appearance of varicocele consists of multiple, serpiginous, tubular structures with varying sizes larger than 2 mm in diameter that are usually best visualized superior and lateral to the testis. Signal intensity characteristics may vary depending on the speed of flow within the dilated vessels. Slow-flowing varicoceles often have intermediate signal intensity on T1-weighted images and high signal intensity on T2-weighted images. A signal void may be seen in those with higher velocity flow. Enhancement is appreciable after gadolinium contrast administration. Since varicocele may affect testicular growth [50], testicular volumes should be systematically measured, and the signal intensity of the parenchyma should be investigated.

9.11 Trauma

If the tunica albuginea is intact, a testicular trauma can be managed conservatively, while immediate operation is usually necessary if albugineal disruption is suspected. MR imaging provides additional clinically useful information in patients with equivocal findings for albugineal disruption on ultrasound. The tunica albuginea is well visualized as a low-signal-intensity line which is interrupted in testicular rupture. In a series of seven patients with blunt scrotal traumas evaluated with MR imaging before surgical exploration, the presence or absence of albugineal rupture was identified correctly in all cases. Associated parenchymal ischemia and hematomas are identified as areas lacking vascularization after gadolinium contrast administration. In testicular hematomas characteristic signal changes with time are appreciated on T1- and T2-weighted images, as methemoglobin within subacute blood is hyperintense on T1-weighted images while hemosiderin deposition produces a low-signal-intensity rim on T2-weighted images. Lack of internal enhancement eases differential diagnosis with hypovascular tumors, which display contrast enhancement after administration of gadolinium contrast material in virtually all cases.

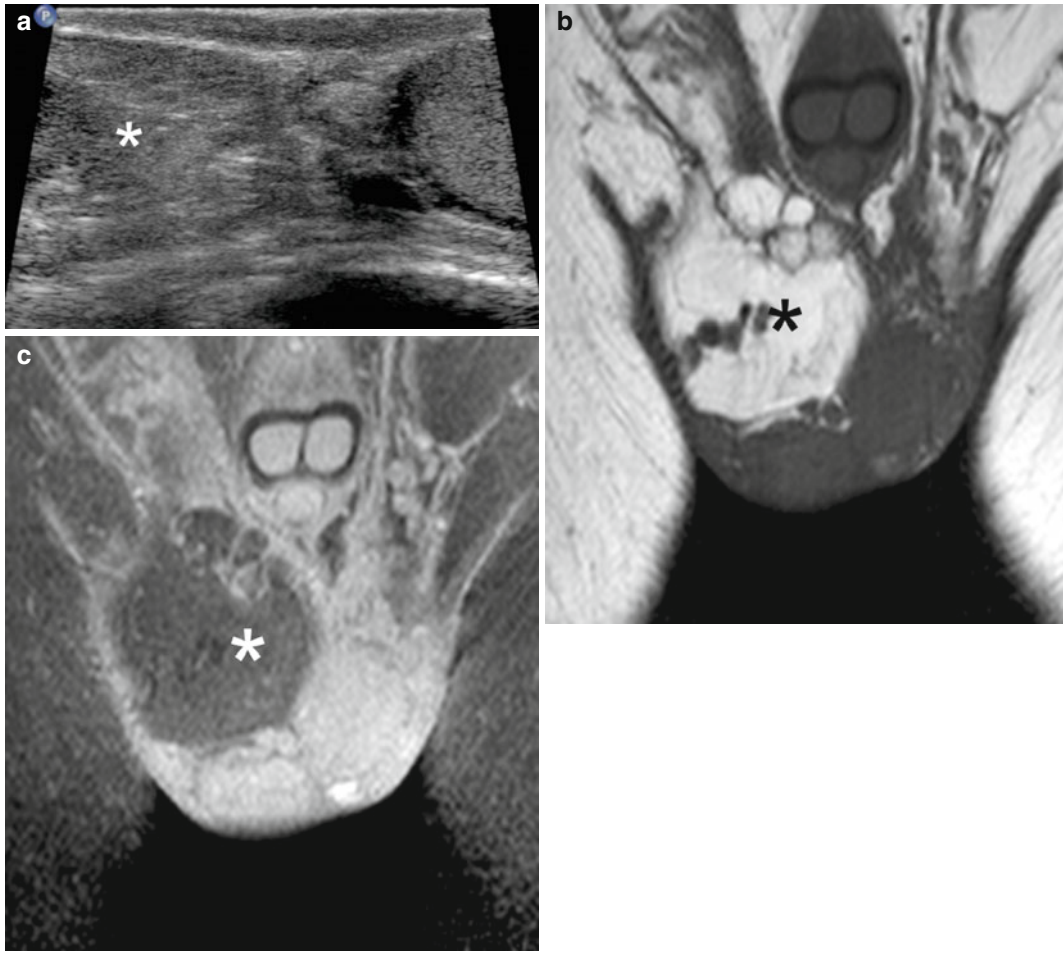

Fig. 9.15 Lipoma of the spermatic cord. (**a**) Grayscale ultrasonography shows a mass (*asterisk*) with intermediate echogenicity involving the spermatic cord. Due to the limited panoramicity, the relationships of the mass cannot be assessed accurately. The lesion (*asterisk*) shows a prevalence of fatty tissue on coronal T1-weighted (**b**) and T1-weighted image with fat suppression (**c**). An adequate evaluation of the relationships with the surrounding tissues is possible

Conclusion

Concern is rising that a variety of scrotal lesions are benign, and surgical exploration can be avoided in many cases, provided that a firm preoperative diagnosis is reached. Ultrasonographic modes have virtually absolute sensitivity for lesion identification, but characterization is limited. Moreover, situations exist in which ultrasonography is inconclusive. Although in the majority of cases the MR appearance of the different intratesticular and extratesticular tumors is not specific, in selected cases MR imaging allows a specific diagnosis based on the identification of fluid or of hematic, fibrotic, and fatty components. Avascular benign lesions can be differentiated effectively from hypovascular tumors due to higher sensitivity of flow compared to color Doppler interrogation.

References

1. Tsili AC, Giannakis D, Sylakos A, Ntorkou A, Sofikitis N, Argyropoulou MI (2014) MR imaging of scrotum. Magn Reson Imaging Clin N Am 22: 217–238, vi
2. Watanabe Y, Dohke M, Ohkubo K et al (2000) Scrotal disorders: evaluation of testicular enhancement patterns at dynamic contrast-enhanced subtraction MR imaging. Radiology 217:219–227

3. Andipa E, Liberopoulos K, Asvestis C (2004) Magnetic resonance imaging and ultrasound evaluation of penile and testicular masses. World J Urol 22:382–391
4. Shellock FG, Rothman B, Sarti D (1990) Heating of the scrotum by high-field-strength MR imaging. AJR Am J Roentgenol 154:1229–1232
5. Rholl KS, Lee JK, Ling D, Heiken JP, Glazer HS (1987) MR imaging of the scrotum with a high-resolution surface coil. Radiology 163:99–103
6. Baker LL, Hajek PC, Burkhard TK et al (1987) MR imaging of the scrotum: normal anatomy. Radiology 163:89–92
7. Frush DP, Sheldon CA (1998) Diagnostic imaging for pediatric scrotal disorders. Radiographics 18:969–985
8. Watanabe Y, Nagayama M, Okumura A et al (2007) MR imaging of testicular torsion: features of testicular hemorrhagic necrosis and clinical outcomes. J Magn Reson Imaging 26:100–108
9. Maki D, Watanabe Y, Nagayama M et al (2011) Diffusion-weighted magnetic resonance imaging in the detection of testicular torsion: feasibility study. J Magn Reson Imaging 34:1137–1142
10. Tsili AC, Argyropoulou MI, Giannakis D, Tsampalas S, Sofikitis N, Tsampoulas K (2012) Diffusion-weighted MR imaging of normal and abnormal scrotum: preliminary results. Asian J Androl 14:649–654
11. Kim MS, Kim KA, Chang SH (2011) Testicular epidermoid cyst on diffusion-weighted MR imaging and ADC map : a case report. J Korean Soc Magn Reson Med 15:154–159
12. Gulum M, Cece H, Yeni E et al (2012) Diffusion-weighted MRI of the testis in hydrocele: a pilot study. Urol Int 89:191–195
13. Kantarci M, Doganay S, Yalcin A, Aksoy Y, Yilmaz-Cankaya B, Salman B (2010) Diagnostic performance of diffusion-weighted MRI in the detection of nonpalpable undescended testes: comparison with conventional MRI and surgical findings. AJR Am J Roentgenol 195:W268–W273
14. Terai A, Yoshimura K, Ichioka K et al (2006) Dynamic contrast-enhanced subtraction magnetic resonance imaging in diagnostics of testicular torsion. Urology 67:1278–1282
15. Tsili AC, Giannakis D, Sylakos A et al (2014) Apparent diffusion coefficient values of normal testis and variations with age. Asian J Androl 16:493–497
16. Kim W, Rosen MA, Langer JE, Banner MP, Siegelman ES, Ramchandani P (2007) US MR imaging correlation in pathologic conditions of the scrotum. Radiographics 27:1239–1253
17. Hricak H, Hamm B, Kim B (1995) Imaging techniques, anatomy, artifacts and bioeffects: magnetic resonance imaging. Raven, New York
18. Nguyen HT, Coakley F, Hricak H (1999) Cryptorchidism: strategies in detection. Eur Radiol 9:336–343
19. Sijstermans K, Hack WW, van der Voort-Doedens LM, Meijer RW (2009) Long-term testicular growth and position after orchidopexy for congenital undescended testis. Urol Int 83:438–445
20. Krishnaswami S, Fonnesbeck C, Penson D, McPheeters ML (2013) Magnetic resonance imaging for locating nonpalpable undescended testicles: a meta-analysis. Pediatrics 131:e1908–e1916
21. Kaipia A, Ryymin P, Makela E, Aaltonen M, Kahara V, Kangasniemi M (2005) Magnetic resonance imaging of experimental testicular torsion. Int J Androl 28:355–359
22. Cassidy FH, Ishioka KM, McMahon CJ et al (2010) MR imaging of scrotal tumors and pseudotumors. Radiographics 30:665–683
23. Gotto GT, Chang SD, Nigro MK (2010) MRI in the diagnosis of incomplete testicular torsion. Br J Radiol 83:e105–e107
24. Baud C, Veyrac C, Couture A, Ferran JL (1998) Spiral twist of the spermatic cord: a reliable sign of testicular torsion. Pediatr Radiol 28:950–954
25. Aso C, Enriquez G, Fite M et al (2005) Gray-scale and color Doppler sonography of scrotal disorders in children: an update. Radiographics 25:1197–1214
26. Dogra VS, Gottlieb RH, Oka M, Rubens DJ (2003) Sonography of the scrotum. Radiology 227:18–36
27. Hricak H, Filly RA (1983) Sonography of the scrotum. Invest Radiol 18:112–121
28. Watanabe Y (2002) Scrotal imaging. Curr Opin Urol 12:149–153
29. Fernandez-Perez GC, Tardaguila FM, Velasco M et al (2005) Radiologic findings of segmental testicular infarction. AJR Am J Roentgenol 184:1587–1593
30. Kodama K, Yotsuyanagi S, Fuse H, Hirano S, Kitagawa K, Masuda S (2000) Magnetic resonance imaging to diagnose segmental testicular infarction. J Urol 163:910–911
31. Saxon P, Badler RL, Desser TS, Tublin ME, Katz DS (2012) Segmental testicular infarction: report of seven new cases and literature review. Emerg Radiol 19:217–223
32. Bertolotto M, Derchi LE, Sidhu PS et al (2011) Acute segmental testicular infarction at contrast-enhanced ultrasound: early features and changes during follow-up. AJR Am J Roentgenol 196:834–841
33. Parenti GC, Feletti F, Brandini F et al (2009) Imaging of the scrotum: role of MRI. Radiol Med 114:414–424
34. Woodward PJ, Sohaey R, O'Donoghue MJ, Green DE (2002) From the archives of the AFIP: tumors and tumorlike lesions of the testis: radiologic-pathologic correlation. Radiographics 22:189–216
35. Langer JE, Ramchandani P, Siegelman ES, Banner MP (1999) Epidermoid cysts of the testicle: sonographic and MR imaging features. AJR Am J Roentgenol 173:1295–1299
36. Park SB, Lee WC, Kim JK et al (2011) Imaging features of benign solid testicular and paratesticular lesions. Eur Radiol 21:2226–2234
37. Gaur S, Bhatt S, Derchi L, Dogra V (2011) Spontaneous intratesticular hemorrhage: two case descriptions and

brief review of the literature. J Ultrasound Med 30: 101–104
38. Hertzberg BS, Mahony BS, Bowie JD, Anderson EE (1985) Sonography of an intratesticular lipoma. J Ultrasound Med 4:619–621
39. Harper M, Arya M, Peters JL, Buckingham S, Freeman A, O'Donoghue EP (2002) Intratesticular lipoma. Scand J Urol Nephrol 36:223–224
40. Serra AD, Hricak H, Coakley FV et al (1998) Inconclusive clinical and ultrasound evaluation of the scrotum: impact of magnetic resonance imaging on patient management and cost. Urology 51: 1018–1021
41. Walker RN, Murphy TJ, Wilkerson ML (2008) Testicular hamartomas in a patient with Bannayan-Riley-Ruvalcaba syndrome. J Ultrasound Med 27: 1245–1248
42. Philips S, Nagar A, Dighe M, Vikram R, Sunnapwar A, Prasad S (2012) Benign non-cystic scrotal tumors and pseudotumors. Acta Radiol 53:102–111
43. Woodhouse J, Ferguson MM (2006) Multiple hyperechoic testicular lesions are a common finding on ultrasound in Cowden disease and represent lipomatosis of the testis. Br J Radiol 79:801–803
44. Liu B, Chen J, Luo J, Zhou F, Wang C, Xie L (2013) Cavernous hemangioma of the testis mimicking a testicular teratoma. Exp Ther Med 6:91–92
45. Tanaka U, Kitajima K, Fujisawa M, Hara S, Takahashi S (2013) Magnetic resonance imaging findings of sclerosing Sertoli cell tumor of the testis. Jpn J Radiol 31:286–288
46. Tsili AC, Tsampoulas C, Giannakopoulos X et al (2007) MRI in the histologic characterization of testicular neoplasms. AJR Am J Roentgenol 189:W331–W337
47. Tsili AC, Argyropoulou MI, Astrakas LG et al (2013) Dynamic contrast-enhanced subtraction MRI for characterizing intratesticular mass lesions. AJR Am J Roentgenol 200:578–585
48. Lee SJ, Lee JH, Jeon SH, Kim MJ (2010) Multiple epidermoid cysts arising from the extratesticular scrotal, spermatic cord and perineal area. Korean J Urol 51:505–507
49. Bertolotto M, Borsato A, Derchi LE (2014) Lymphoma of the spermatic cord: Sonographic appearance. J Clin Ultrasound 42:509-512
50. Thomas JC, Elder JS (2002) Testicular growth arrest and adolescent varicocele: does varicocele size make a difference? J Urol 168:1689–1691